Magnetic field sensor based on dual S-tapered multimode fiber interferometer

Xu Zhang[1], Bo Liu[1], Hao Zhang[1], Jixuan Wu[1], Binbin Song[2] and Chao Wang[3]

[1] Key Laboratory of Optical Information Science and Technology, Ministry of Education, Tianjin Key Laboratory of Optoelectronic Sensor and Sensing Network Technology, Institute of Modern Optics, Nankai University, Tianjin 300350, China

[2] Key Laboratory of Computer Vision and Systems, Ministry of Education, School of Computer Science and Engineering, Tianjin University of Technology, Tianjin 300384, China

[3] School of Engineering and Digital Arts, University of Kent, Canterbury, United Kingdom CT2 7NT

E-mail: liubo@mail.nankai.edu.cn

Abstract

A multimode interferometer (MMI) for the measurement of magnetic field based on concatenated S-tapered fibers is proposed and experimentally demonstrated. Spectrally interrogated magnetic field sensing is achieved by integrating the proposed MMI with magnetic fluids. The magnetic sensitivity of the MMI reaches 0.011 dB/Oe. Owing to its desirable advantages such as compactness, low cost, fast response and flexible structure, the proposed MMI is anticipated to find potential applications in in-situ measurement of magnetic field.

Keywords: multimode interferometer, magnetic field sensing, magnetic fluids, in-situ measurement.

1. Introduction

Magnetic fluids (MFs) is one kind of magneto-optical nano-material constituted by surfactant-coated magnetic nanoparticles suspending in carrier fluids [1]. Under external magnetic fields, MFs would exhibit versatile physical properties, including Faraday and birefringence effect, tunable

refractive index, thermal-optical effect, optical anisotropy, and field-dependent transmission, etc [2-6]. And in recent years, MFs has been applied as functional materials in various photonic devices such as magneto-optical modulators [6, 7], optical switches [8], tunable optical capacitors [9], tunable filters [10], and magnetic field sensors [11-24], etc.

In particular, magnetic field sensors have found various applications in the fields of scientific research and civil engineering. With the rapid development of fiber photonics, fiber-optic magnetic field sensors have been intensively studied for their compact size, rapid response, immunity to electromagnetic interference, and corrosion resistance. Due to the refractive index tunability of MFs under external magnetic field, various optical fiber structures have been functionalized with MFs to achieve magnetic field sensors, including fiber gratings [11-13], micro-fiber structures [14-17], no-core fiber (NCF) [18, 19], thin-core fiber (TCF) [20, 21], and MF-infiltrated photonic crystal fibers (PCF) or hollow core fiber (HCF) [22-24]. In addition, fiber interferometers functionalized with MFs have also been developed for the magnetic field sensing [25-28]. Xia et al. proposed a fiber Fabry-Perot cavity with a fiber Bragg grating written in the lead-in fiber to achieve simultaneous detection of the magnetic field and temperature [27]. Li et al. proposed a magnetic field sensor by employing a twin-core-fiber-based compact in-fiber Mach–Zehnder interferometer [28].

Recently the S-tapered fiber interferometer has attracted growing research interest and a good variety of S-tapered fiber sensors have been developed for the measurement of different physical or chemical parameters such as temperature [29], refractive index [30], strain [31], and humidity [32], etc. An in-line Mach–Zehnder interferometer (MZI) based on two S-bend fibers has been proposed to measure the displacement and force in the meantime [33]. However, due to the slight difference between of waist diameters of S-tapered fibers and single mode fiber (SMF), the RI sensitivity of their proposed fiber interferometer is relatively low.

To solve the above issue, in this paper a MMI based on concatenated thin-waist S tapers is proposed and experimentally investigated. The two S-tapered fibers are simply fabricated by using a commercial fusion splicer with off-axis pulling mode to enhance the evanescent field and the length of the SMF between two S tapers is 9 mm. Owing to the multimodal interference induced by the mode field mismatch between the S-taper fibers and SMF, the transmission loss of the proposed MMI is sensitive to the applied magnetic field intensity. The proposed MMI has compact size, low

cost, fast response and flexible structure, which make it a promising candidate for practical magnetic field sensing applications.

2. Experimental setup and operation principle

The experimental setup for magnetic field sensing system based on concatenated S-tapered MMI is shown in Fig. 1, which consists of a broadband source (BBS, wavelength ranges 1250 nm to 1640 nm), an optical spectrum analyzer (OSA: Yokogawa AQ6370C, operation wavelength ranges from 600 nm to 1700 nm) with a resolution of 0.5 nm, two electromagnets, and a tunable voltage source (TVS). The electromagnetic field produced by the TVS and applied in perpendicular to the fiber axis. The magnetic field intensity is measured by using a Tesla meter with a resolution of 0.1 Oe. The sensing region is kept straight by a fiber holder and a rotator and then encapsulated into a capillary with an inner diameter of 300 μm. By exploiting capillarity force, the capillary is filled with MFs (EMG605, Ferrotec, Inc.). Both ends of the capillary tube are sealed with paraffin to avoid the leakage of MFs during the experimental process.

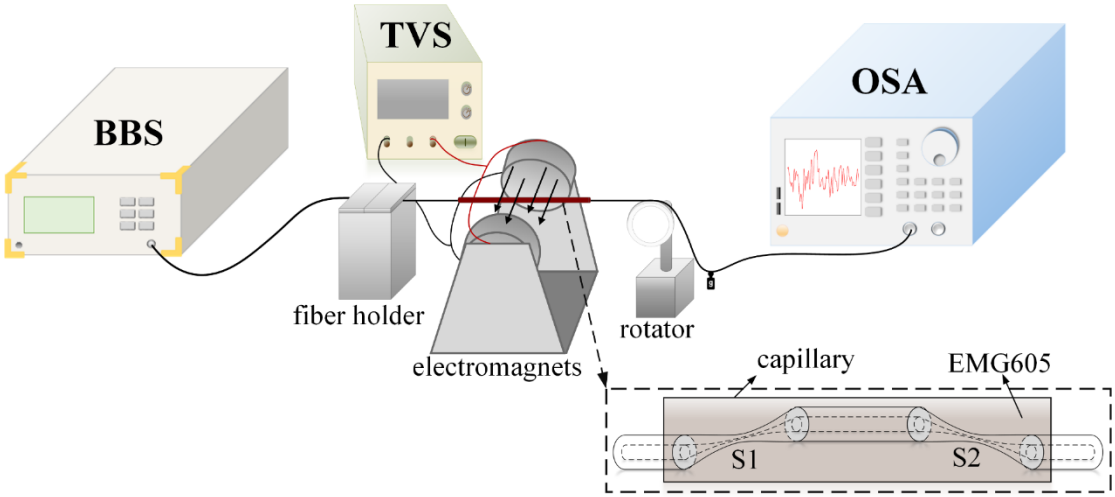

Figure 1. Schematic diagram of the experimental setup for concatenated S-tapered MMI integrated with MFs.

Two S tapers are fabricated by using a commercial fusion splicer. The fabrication procedure of the MMI structure is shown in Fig. 2. A segment of SMF (SMF-28e) is clamped by fusion splicer clamps to keep it straight, as shown in Fig. 2 (a). Subsequently, one fiber clamp is manually

controlled to obtain some axial offset and a "clean" arc charge is performed to form an S taper, as shown in Fig. 2 (b). The waist diameter of the S-taper could be further reduced by moving the clamps outward with minimum step size and applying discharge for a second time. This procedure is repeated 5 to 6 times. After that, as shown in Fig. 2 (c) and (d), the fiber is cut off by using a fiber cleaver at the other end about 4 to 5 mm from the taper region, and then is spliced with another S-taper fabricated in the same way. Fig. 3 gives the microscopic images of the two fabricated S-tapered fibers. The geometrical parameters of two S tapers are as follows: waist diameter W_1=67.27 μm, W_2=64.83 μm; length L_1=471.48 μm, L_2=471.92 μm; axial offset D_1=72.16 μm, D_2=54.26 μm. The length of the SMF between two S-tapered fibers is 9 mm.

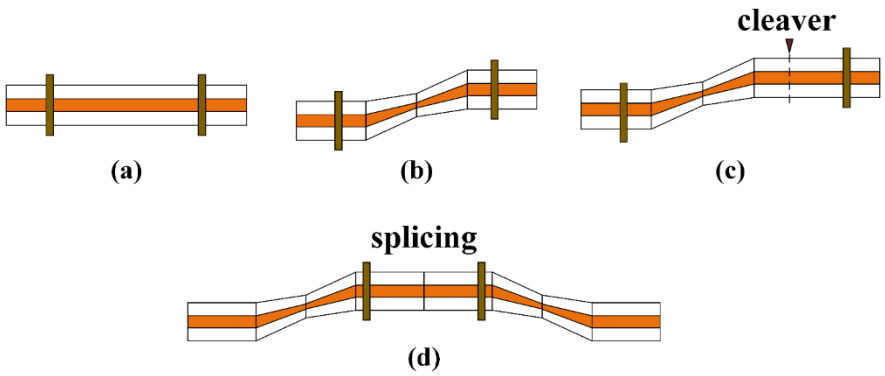

Figure 2. Schematic illustration for the fabrication procedure of the concatenated S-tapered MMI. (a) and (b) fabrication procedure of S-tapered fibers; (c) and (d) fabrication procedure of the MMI with one segment of SMF between two S tapers.

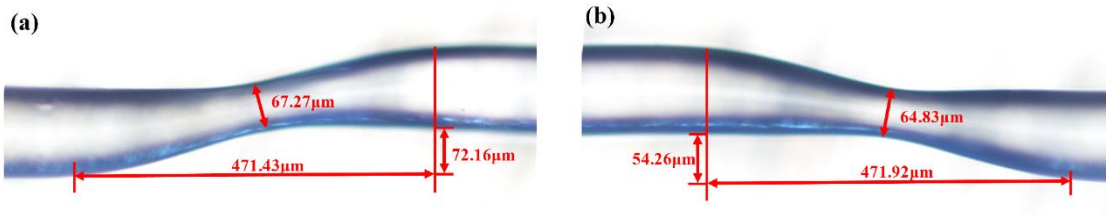

Figure 3. Microscopic images of the two fabricated S-tapered fibers. (a) S-tapered fiber S1 (b) S-tapered fiber S2.

For a single S-tapered fiber, high-order cladding modes are excited at the first fiber taper. When the input light propagates through the second coupling region, the core mode and cladding modes

will interfere due to the presence of difference in optical paths [34]. The interferometric dip wavelength λ_m can be expressed as:

$$\lambda_m = 2\Delta n_{eff} L/(2m+1) \quad (1)$$

where n_{eff} is the effective refractive index difference between the core and the cladding modes, L is the effective length of the S-tapered region, and m is the interference order. Fig. 4 (a) shows the transmission spectra of the two S-tapered fibers, and fig. 4 (b) shows the Fourier frequency spectra of these two S-tapered fibers. It can be seen that, besides the fundamental frequency there is only one main frequency component in the Fourier frequency spectra of a single S-tapered fiber interferometer, and therefore it could be regarded as a two-mode fiber interferometer with a periodic interferometric spectrum.

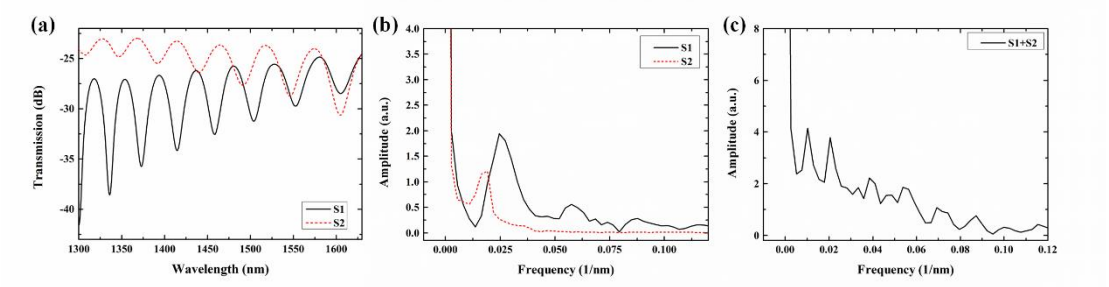

Figure 4. Transmission spectra of the two single S-tapered fiber interferometers; (b) Fourier frequency spectra of the two single S-tapered fiber interferometers; (c) Fourier frequency spectrum of the concatenated S-tapered fiber interferometer.

When SMF is spliced with the two S-tapered fibers in between, the concatenated structure can be regarded as a multimode waveguide. Multitude of high order cladding modes would be excited at the lead-in S-tapered fiber. Meanwhile the light propagating through the fiber core is still operating in single mode. In the lead-out S-tapered region, some of the high order cladding modes could be coupled back into the fundamental core mode. Due to the difference in propagation constants for different high order cladding modes, multitude of cladding modes and the fundamental mode in fiber core would interference with each other and multimodal interference would occur as light propagates through the S-tapered fibers in turn. And thus interferometric transmission spectrum can be obtained at output of the dual S-tapered fiber structure. As shown in fig. 4 (c), frequency components of the modes participating in the modal interference are quite complex, causing the

interference spectrum to deviate from standard period pattern. Assume the total length of the MMI is z, the output transmission of light can be written as:

$$I_{out} = \left|E\left(x,y\right)\right|^2 = \left|\sum_{m=0}^{M} a_m \psi_m\left(x,y\right)\exp(j\beta_m z)\exp\left(-\gamma_m z\right)\right|^2 \tag{2}$$

where E is the superposition of field profile, M is the number of the optical modes that participate in multimodal interference, a_m, ψ_m, β_m and γ_m are the excitation coefficient, field profile, propagation constant and the evanescent absorption coefficient, respectively.

When the proposed sensor is immersed in MFs, the evanescent absorption coefficient γ_m can be written as [35]

$$\gamma_m = \frac{\alpha_\lambda \lambda n_{MF} \cos\theta_m \cot\theta_m}{4\pi a n_c^2 \cos^2\theta_c \sqrt{\sin^2\theta_m - \sin^2\theta_c}} \tag{3}$$

where λ is the wavelength in vacuum, α_λ is attenuation coefficient of the cladding material (MFs in our experiment) at wavelength of λ, n_{MF} and n_c are the refractive indices of the MFs and fiber cladding, respectively. a is fiber radius. θ_c is critical angle, which can be calculated by

$$\theta_c = \sin^{-1}\left(\frac{n_{MF}}{n_c}\right) \tag{4}$$

And $\theta_m = \sin^{-1}\left(\frac{\beta_m}{k}\right)$, where $k = \frac{2\pi n_c}{\lambda}$ is the wave number.

When certain magnetic field is applied, magnetic particles will be magnetized to form a nanochain-like structure paralleled to the field direction [36]. Phase separation will occur during this process, causing the variation in effective dielectric constant [37]. The relationship between refractive index n_{MF} and effective dielectric constant ε_{MF} is shown by [38]

$$n_{MF} = \sqrt{\varepsilon_{MF}} \tag{5}$$

The effective dielectric constant ε_{MF} of the MF film can be expressed as [37]

$$\varepsilon_{MF} = \frac{-\varepsilon_{col}\left(1-f\right) - \varepsilon_{liq}\left(f-1\right) + \sqrt{\left[\varepsilon_{col}\left(1-f\right) + \varepsilon_{liq}\left(f-1\right)\right]^2 + 4\left(1+f\right)^2 \varepsilon_{col}\varepsilon_{liq}}}{2\left(1+f\right)} \tag{6}$$

where ε_{col} and ε_{liq} represent the dielectric constant of the magnetic column and the liquid phase, respectively. ε_{col} maintains constant, but ε_{liq} varies with the magnetic-field strength. $f = (A_{col} / A) / (1 - A_{col} / A)$, where A_{col} / A represents the area occupied by the magnetic columns, which is dependent on the external magnetic field. Thus according to Eq. (5) and Eq. (6), the refractive index n_{MF} is dependent on the strength of applied magnetic field.

The presence of applied magnetic field affects the refractive index n_{MF}, leading γ_m and β_m to change [35]. According to Eq. (2), the change of the magnetic field intensity can be detected by the output transmission intensity.

Fig. 5 shows the simulated light propagation through the dual S-tapered fiber structure based on beam propagation theory (BPM). Insets give enlarged two S taper regions. From the simulation results, it is apparent that the evanescent field around the two S taper regions are significantly strong, which makes the transmission spectral characteristics sensitive to the refractive index of external medium.

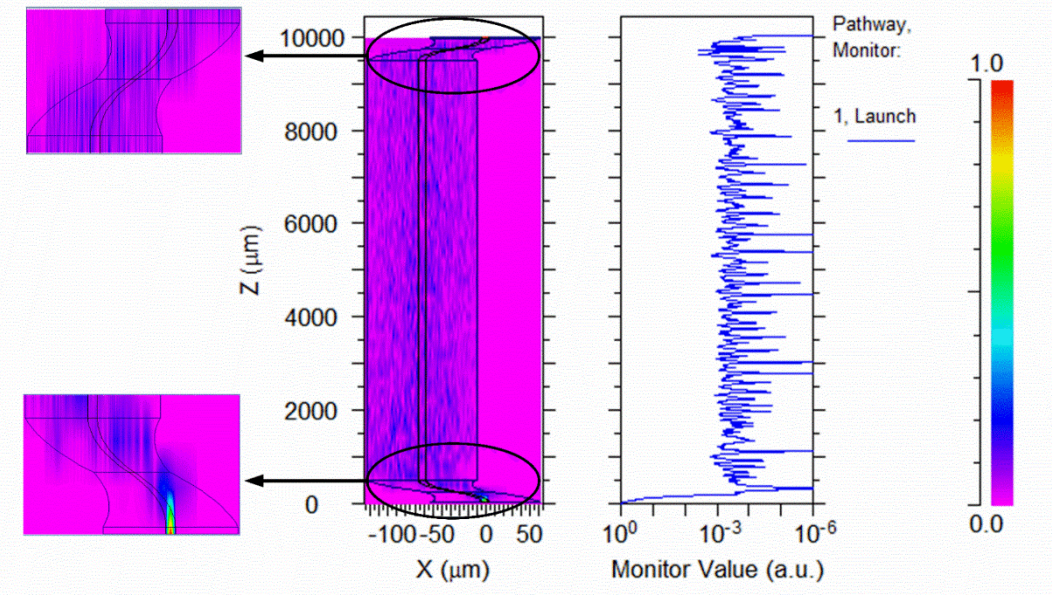

Figure 5. Simulated electric amplitude distribution of the MMI with 9 mm SMF between two S-tapered fibers.

3. Experimental results and discussion

All of the experiments were conducted under a constant room temperature of 25.9℃. Fig. 6 shows the transmission spectra of the MMI exposed in air and immersed into MFs, respectively. Due to the strong absorption and scattering of MFs as well as the variation in environmental refractive, transmission spectra of the concatenated structure changes accordingly.

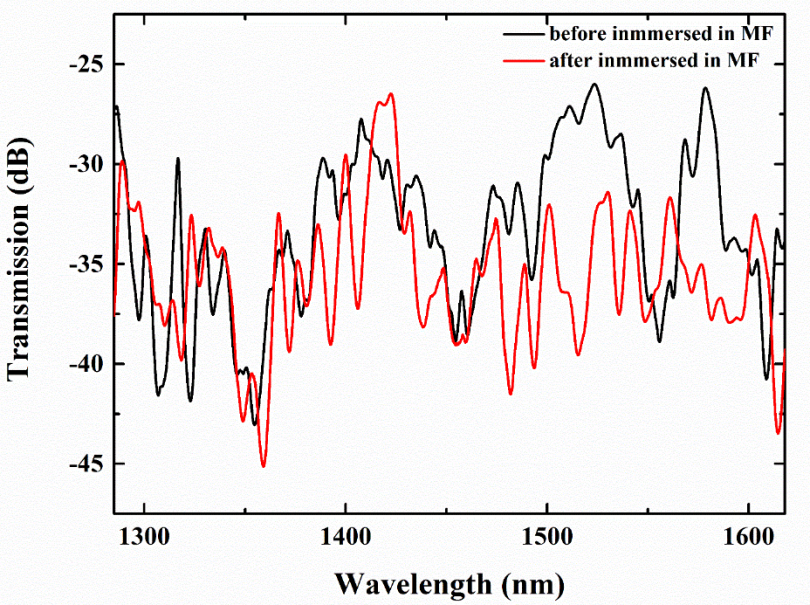

Figure 6. Transmission spectra of the MMI before and after being immersed into MFs.

Fig. 7 shows the transmission spectra of the MMI under different applied magnetic field. As magnetic field intensity increases from 0 Oe to 500 Oe, the magnetic fluid nanoparticles tend to agglomerate to form magnetic chain-like clusters. Thus the refractive index of MF will change with the magnetic field intensity, causing the increment of spectral transmission loss.

Fig. 8 gives transmission spectral responses of dip A and dip B to the change of applied magnetic field intensity. Due to the initial magnetization, the transmission spectral intensity slightly changes when the magnetic field intensity is below 50 Oe. And because of saturated magnetization of the MFs, transmission spectral intensity tends to maintain unchanged when applied magnetic field intensity is higher than 300 Oe. As magnetic field intensity increases from 0 Oe to 500 Oe, the transmission intensity increases from -42.743 dB and -39.077 dB to -38.944 dB and -37.029 dB for dip A and dip B, respectively. It should be noted that as applied magnetic field intensity lies between 75 Oe and 250 Oe, transmission intensities for the above two dips both linearly vary with the magnetic field intensity. The magnetic sensitivity and coefficient of determination reach 0.011

dB/Oe and 0.98167 for dip A and 0.007 dB/Oe and 0.99541 for dip B, respectively.

A comparison of performances between our proposed concatenated S-tapered fiber sensor and other fiber-based structures is summarized in Table 1. It can be seen that compared with other sensor structures, our proposed magnetic field sensor is more compact but shows the same order of magnitude in terms of magnetic field sensitivities and measurement range. And moreover, our proposed sensor is based on SMF with no need of core offset splicing and the diameters of the tapered regions are still larger than 60 μm, which make this sensor easier to fabricate, more economical and more robust. It is worth noting that the sensitivity of the proposed concatenated S-tapered fiber sensor could be further improved by reducing the taper diameter and increasing the fluid interaction length.

Table 1. Sensor performances of the proposed concatenated S-tapered fiber interferometer in comparison with other fiber-optic magnetic field sensors

Sensor structure	Detection sensitivity (dB/Oe)	Detection range (Oe)	Sensor size (mm)	Reference
Microfiber coupler	-0.037	50-275	~10	[17]
MSM Fiber Structures	0.05742	20-140	30	[25]
Up-Tapered Joints	-0.02121	20-300	14	[39]
Core-offset tapered fiber	0.03407	100-300	20	[40]
Core-Offset Microfiber	0.01111	128-564	20	[41]
Our proposed fiber sensor	0.011	100-250	9	

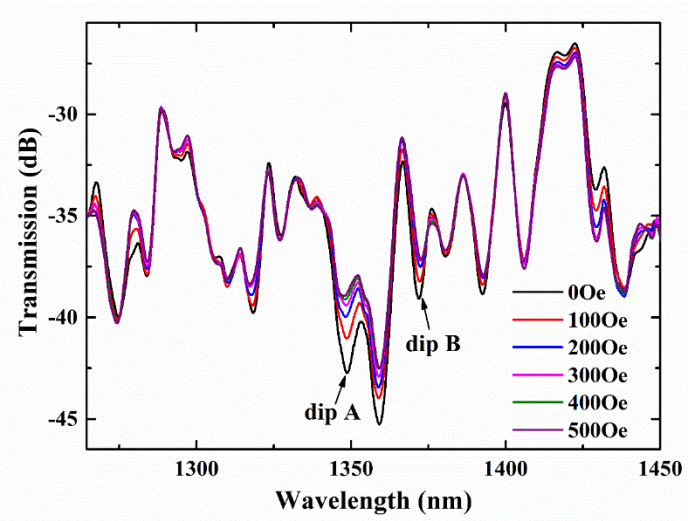

Figure 7. Transmission spectral evolution of the MMI under different applied magnetic field

intensities

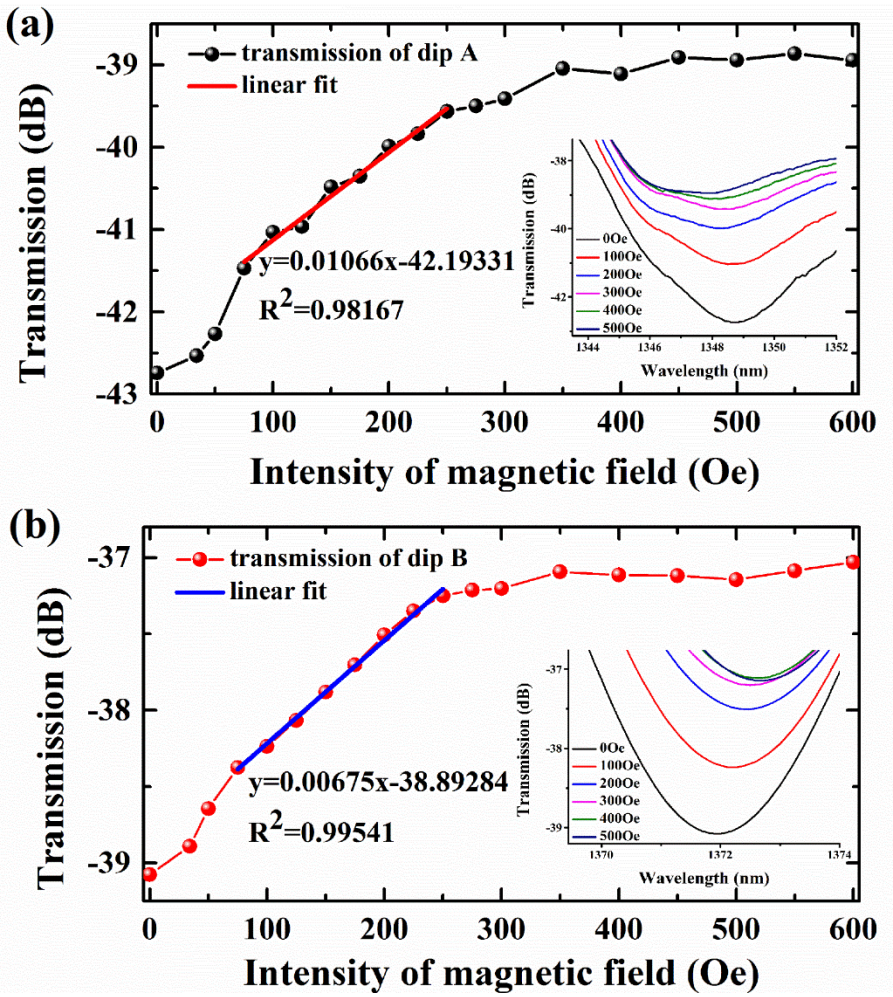

Figure 8. Transmission intensity as functions of applied magnetic field intensity for (a) dip A and (b) dip B, respectively.

4. Conclusion

A magnetic field sensor based on concatenated S-tapered fiber MMI integrated with MFs has been proposed and experimentally demonstrated. Experimental results indicate that the transmission spectral intensity of the proposed MMI is sensitive to the change of applied magnetic field intensity, and linear sensing curve has been experimentally acquired for a magnetic field intensity range of 100 Oe to 250 Oe. The performances of the proposed magnetic field sensor can be further improved by optimizing the geometrical parameters of S-tapered fibers. Owing to its advantages such as

compactness, low cost, fast response and flexible structure, the proposed MMI sensor provides a promising candidate for the measurement of magnetic field intensity in practical applications.

Acknowledgments

This work was jointly supported by the National Natural Science Foundation of China under Grant Nos. 61377095, 11774181, 11274182, and 11004110, the 863 National High Technology Program of China under Grant No. 2013AA014201, Science & Technology Support Project of Tianjin under Grant No. 16YFZCSF00400, and the Fundamental Research Funds for the Central Universities.

References

[1] Zhao Z, Tang M, Gao F, Zhang P, Duan L, Zhu B, Fu S, Ouyang J, Wei H, Li J, Shum PP and Liu D 2014 Temperature compensated magnetic field sensing using dual S-bend structured optical fiber modal interferometer cascaded with fiber Bragg grating *Opt. Express* **22** 27515-23

[2] Zu P, Chan CC, Siang LW, Jin Y, Zhang Y, Fen LH, Chen L and Dong X 2011 Magneto-optic fiber Sagnac modulator based on magnetic fluids *Opt. Lett*. **36** 1425-7.

[3] Horng HE, Hong CY, Yang SY and Yang HC 2003 Designing the refractive indices by using magnetic fluids *Appl. Phys. Lett* **82** 2434-6.

[4] Pu S, Chen X, Liao W, Chen L, Chen Y and Xia Y 2004 Laser self-induced thermo-optical effects in a magnetic fluid *J. Appl. Phy.* **96** 5930-2.

[5] Miao Y, Liu B, Zhang K, Liu Y and Zhang H 2011 Temperature tunability of photonic crystal fiber filled with Fe3O4 nanoparticle fluid *Appl. Phys. Lett.* **98** 021103.

[6] Pu S, Chen X, Chen Y, Xu Y, Liao W, Chen L and Xia Y 2006 Fiber-optic evanescent field modulator using a magnetic fluid as the cladding *J. Appl. Phy.* **99** 093516.

[7] Horng HE, Chieh JJ, Chao YH, Yang SY, Hong CY and Yang HC 2005 Designing optical-fiber modulators by using magnetic fluids *Opt. Lett*. **30** 543-5.

[8] Horng HE, Chen CS, Fang KL, Yang SY, Chieh JJ, Hong CY and Yang HC 2004 Tunable optical switch using magnetic fluids *Appl. Phys. Let*. **85** 5592-4.

[9] Patel R and Mehta RV 2011 Ferrodispersion: a promising candidate for an optical capacitor *Appl. Optics* **50** G17-G22.

[10] Liao W, Chen X, Chen Y, Pu S, Xia Y and Li Q 2005 Tunable optical fiber filters with magnetic fluids *Appl. Phys. Let* **87** 151122.

[11] Candiani A, Konstantaki M, Margulis W and Pissadakis S 2010 A spectrally tunable microstructured optical fibre Bragg grating utilizing an infiltrated ferrofluid *Opt. Express.* **18** 24654-60.

[12] Zheng J, Dong X, Zu P and Ji J 2013 Intensity-modulated magnetic field sensor based on magnetic fluid and optical fiber gratings *Appl. Phys. Let.* **103** 183511.

[13] Dai J, Yang M, Li X, Liu H and Tong X 2011 Magnetic field sensor based on magnetic fluid clad etched fiber Bragg grating *Opt. Fiber Technol.* **17** 210-3.

[14] Miao Y, Wu J, Lin W, Zhang K, Yuan Y, Song B, Zhang H, Liu B and Yao J 2013 Magnetic field tunability of optical microfiber taper integrated with ferrofluid. *Opt. Express*. **21** 29914-20.

[15] Zheng Y, Dong X, Chan CC, Shum PP and Su H 2015 Optical fiber magnetic field sensor based on magnetic fluid and microfiber mode interferometer *Opt. Commun*. **336** 5-8.

[16] Luo L, Pu S, Tang J, Zeng X and Lahoubi M 2015 Reflective all-fiber magnetic field sensor based on microfiber and magnetic fluid. *Opt. Express*. **23** 18133-42.

[17] Luo L, Pu S, Tang J, Zeng X and Lahoubi M 2015 Highly sensitive magnetic field sensor based on microfiber coupler with magnetic fluid. *Appl. Phys. Let.* **106** 193507

[18] Chen Y, Han Q, Liu T, Lan X and Xiao H 2013 Optical fiber magnetic field sensor based on single-mode–multimode–single-mode structure and magnetic fluid *Opt. Lett*. **38** 3999-4001.

[19] Lin W, Miao Y, Zhang H, Liu B, Liu Y and Song B 2013 Fiber-optic in-line magnetic field sensor based on the magnetic fluid and multimode interference effects *Appl. Phys. Let.* **103** 151101.

[20] Wu J, Miao Y, Song B, Lin W, Zhang H, Zhang K, Liu B and Yao J 2014 Low temperature sensitive intensity-interrogated magnetic field sensor based on modal interference in thin-core fiber and magnetic fluid *Appl. Phys. Let.* **104** 252402.

[21] Zhang J, Qiao X, Yang H, Wang R, Rong Q, Lim K-S and Ahmad H 2017 All-fiber magnetic field sensor based on tapered thin-core fiber and magnetic fluid *Appl. Optics* **56** 200-4.

[22] Gao R, Jiang Y and Abdelaziz S 2013 All-fiber magnetic field sensors based on magnetic fluid-filled photonic crystal fibers *Opt. Lett*. **38** 1539-41.

[23] Li J, Wang R, Wang J, Zhang B, Xu Z and Wang H 2014 Novel magnetic field sensor based on

magnetic fluids infiltrated dual-core photonic crystal fibers *Opt. Fiber Technol.* **20** 100-5.

[24] Song B, Miao Y, Lin W, Zhang H, Liu B, Wu J, Liu H and Yan D 2014 Loss-based magnetic field sensor employing hollow core fiber and magnetic fluid *IEEE Photonic. Tech. L.* **26** 2283-6.

[25] Tang J, Pu S, Dong S and Luo L 2014 Magnetic field sensing based on magnetic-fluid-clad multimode-singlemode-multimode fiber structures *Sensors* **14** 19086-94.

[26] Dong S, Pu S and Wang H 2014 Magnetic field sensing based on magnetic-fluid-clad fiber-optic structure with taper-like and lateral-offset fusion splicing *Opt. Express.* **22** 19108-16.

[27] Ji X, Wang F, Hong L, Qi W and Xiong S 2016 A Magnetic Field Sensor Based on a Magnetic Fluid-Filled FP-FBG Structure *Sensors* **16** 620.

[28] Li Z, Liao C, Song J, Wang Y, Zhu F and Dong X 2016 Ultrasensitive magnetic field sensor based on an in-fiber Mach-Zehnder interferometer with a magnetic fluid component *Photonics Res*. **4** 197-201.

[29] Li J, Zhang W, Gao S, Geng P, Xue X, Bai Z and Liang H 2013 Long-Period Fiber Grating Cascaded to an S Fiber Taper for Simultaneous Measurement of Temperature and Refractive Index *IEEE Photonic. Tech. L.* **25** 888-91.

[30] Shi F, Wang J, Zhang Y, Xia Y and Zhao L 2013 Refractive Index Sensor Based on S-Tapered Photonic Crystal Fiber *IEEE Photonic. Tech. L* **25** 344-7.

[31] Yang R, Yu Y, Chen C, Xue Y, Zhang X, Guo J, Wang C, Zhu F, Zhang B, Chen Q and Sun H 2012 S-Tapered Fiber Sensors for Highly Sensitive Measurement of Refractive Index and Axial Strain *J. Lightwave Technol.* **30** 3126-32.

[32] Liu H, Miao Y, Liu B, Lin W, Zhang H, Song B, Huang M and Lin L 2015 Relative Humidity Sensor Based on S-Taper Fiber Coated With SiO2 Nanoparticles. *IEEE Sen. J.* **15** 3424-8.

[33] Chen J, Zhou J and Yuan X 2014 M–Z Interferometer Constructed by Two S-Bend Fibers for Displacement and Force Measurements *IEEE Photonic. Tech. L* **26** 837-40.

[34] Yang R, Yu Y-S, Xue Y, Chen C and Chen Q-D 2011 Sun H-B. Single S-tapered fiber Mach–Zehnder interferometers *Opt. Lett*. **36** 4482-4.

[35] Ding X, Yang H, Qiao X, Zhang P, Tian O, Rong Q, Nazal N, Lim K and Ahmad H 2018 Mach–Zehnder interferometric magnetic field sensor based on a photonic crystal fiber and magnetic fluid *Appl. Optics* **57** 2050-6.

[36] Yin J, Yan P, Chen H, Yu L, Jiang J, Zhang M and Ruan S 2017 All-fiber-optic vector magnetometer based on anisotropic magnetism-manipulation of ferromagnetism nanoparticles *Appl. Phys. Let.* **110** 231104.

[37] Yang SY, Chieh JJ, Horng HE, Hong CY and Yang HC 2004 Origin and applications of magnetically tunable refractive index of magnetic fluid films *Appl. Phys. Let.* **84** 5204-6.

[38] Horng HE, Chieh JJ, Chao YH, Yang SY, Hong CY and Yang HC 2005 Designing optical-fiber modulators by using magnetic fluid *Opt. Lett.* **30** 543-5.

[39] Pu S and Dong S 2014 Magnetic Field Sensing Based on Magnetic-Fluid-Clad Fiber-Optic Structure With Up-Tapered Joints *IEEE Photonics J.* **6** 1-6.

[40] Wu J, Miao Y, Lin W, Song B, Zhang K, Zhang H, Liu B and Yao J 2014 Magnetic-field sensor based on core-offset tapered optical fiber and magnetic fluid *J. Optics* **16** 2433-9.

[41] Wu J, Miao Y, Lin W, Zhang K, Song B, Zhang H, Liu.B and Yao J 2014 Dual-Direction Magnetic Field Sensor Based on Core-Offset Microfiber and Ferrofluid. *IEEE Photonic. Tech. L.* **26** 1581 - 4.